Received: 22 October 2021 | Revised: 26 July 2022 | Accepted: 27 July 2022

DOI: 10.1002/acs.3478

RESEARCH ARTICLE

WILEY

Output-feedback boundary adaptive fault-tolerant control for scalar hyperbolic partial differential equation systems with actuator faults

Runsheng Guo | Jiachen Li | Kangkang Sun | Tong Wang | Jianbin Qiu

Research Institute of Intelligent Control and Systems, Harbin Institute of Technology, Harbin, China

Correspondence
Tong Wang, Research Institute of Intelligent Control and Systems, Harbin Institute of Technology, Harbin 150080, China.
Email: twang@hit.edu.cn

Funding information
National Natural Science Foundation of China, Grant/Award Numbers: U21B6001, 62173109, 61873311; Special Project of Heilongjiang Postdoctoral Science Foundation, Grant/Award Number: LBH-TZ2011; 111 Project, Grant/Award Number: B16014

Summary

This article studies the output-feedback adaptive fault-tolerant boundary control problem for scalar hyperbolic partial differential equation systems with actuator faults. All the coefficients of the controlled plant are unknown, and two types of actuator faults, that is, multiplicative faults and additive faults, are considered simultaneously. For the state estimation problem, two filters are constructed, based on which an observer is obtained to estimate the system state. A parametric model is established for actuator faults, based on which the parameter updating laws of gradient type are then developed to identify actuator faults and to estimate the unknown system coefficients. With the observer and the parameter updating laws, an output-feedback adaptive fault-tolerant boundary control law is developed via infinite-dimensional backstepping method. The boundness of all the signals involved in the control design is guaranteed and the convergence of system states is also confirmed. Finally, the simulation results are given to testify the effectiveness of the proposed control scheme.

KEYWORDS

actuator faults, adaptive control, boundary control, fault-tolerant control, hyperbolic PDE systems

1 | INTRODUCTION

With the rapid development of science and technology, the complexity of modern control system is increasing which often leads to the failures of control systems. To reduce the impact caused by system faults and improve the reliability of control systems, fault-tolerant control (FTC) problems[1-7] have been extensively investigated during the past decades. In general, FTC strategies can be categorized into two groups: passive control strategy[8-10] and active control strategy.[11,12] For the former case, the robust control strategy is proposed which is capable of accommodating all the possible system faults. Whereas the control performance may degrade due to the conservatism of the control strategy.[13] For the latter case, fault detection and diagnosis (FDD) modules are applied and the control law is reconfigured to accommodate system faults. Obviously, with active control strategy, the control systems are capable of obtaining better performance.[13] Moreover, among active control strategies, adaptive FTC strategy is widely utilized due to the fact that all the system uncertainties, including system faults and uncertain parameters, can be compensated via adaptive techniques. For example, the authors in Reference 14 proposed an adaptive FTC scheme to compensate two types of actuator faults as well as uncertain parameters simultaneously for a time-varying system. The authors in Reference 15 proposed an adaptive sliding mode control scheme to address the FTC problem for an aircraft system with both system uncertainties and actuator saturation. Furthermore, the authors in References 16-23 addressed the FTC issues for several nonlinear systems via adaptive neural-network control and adaptive fuzzy control strategies, respectively.

Note that only the control systems described by ordinary differential equation (ODE) are considered in the aforementioned results. In practice, various physical phenomena can be described by partial differential equation (PDE) systems, such as fluid flows, flexible structures, chemical process in industries, and so on.[24,25] Therefore, the control issues of PDE systems have also been extensively investigated during the past decades. The authors in References 26-32 studied the boundary control issues of PDE systems via infinite-dimensional backstepping method, and various PDE systems were considered, such as parabolic PDE systems,[26,27] hyperbolic PDE systems,[28,29] Euler–Bernoulli beam (EBB) systems,[30] and so on.[31,32] Moreover, based on the infinite-dimensional backstepping method, fruitful results have also been obtained for the adaptive control problem via different approaches such as Lyapunov's direct approach,[33,34] estimation based approach,[35] and swapping identifiers based approach.[36-38] For the aforementioned literatures, the boundary control problems of PDE systems were investigated only for the fault-free case.

More recently, the FTC problems of PDE systems have also been considered. The authors in Reference 39 investigated the FTC problems for a 3D EBB system, in which an adaptive FTC scheme was proposed to compensate actuator faults. The authors in Reference 40 investigated the FTC issue for a class of nonlinear parabolic PDE systems with actuator faults, in which the observer-based fuzzy in-domain FTC law was proposed to accommodate actuator faults. Moreover, by incorporating in-domain control strategy, FDD and FTC strategies for PDE systems with actuator faults were proposed in Reference 41. Moreover, the FTC problem for PDE systems with the constant actuator/sensor faults has attracted researchers' attention. In Reference 42, a robust FTC scheme was proposed for a class of cascaded ODE-EBB systems with constant actuator faults, uncertain coefficients and disturbances. In Reference 43, a fault estimation approach was proposed for a class of hyperbolic PDE systems with both constant actuator and sensor faults. In Reference 44, a model-based fault estimation and prediction method was proposed for a class of parabolic PDE systems with both constant actuator and sensor faults. However, most of the aforementioned results are for FTC issues of EBB systems or parabolic PDE systems.

Motivated by the previous discussions, this article investigates the output-feedback boundary adaptive FTC for scalar hyperbolic PDE system with constant actuator faults. In this article, challenges from three different aspects are considered simultaneously for scalar hyperbolic PDE systems, that is, (i) unknown spatially varying parameters, (ii) boundary measurement, (iii) combined multiplicative and additive actuator faults. Compared with the existing result, the contributions of this article are listed as follows:

(i) The combined multiplicative and additive actuator faults are both considered in this article.
(ii) Compared with the results in Reference 45, the controlled plant in this article is more complicated, and multiplicative actuator faults are also considered.
(iii) In the existing results, the FTC issues of PDE systems are mostly addressed via Lyapunov's direct approach. In this article, parameter updating laws of gradient type are developed to compensate actuator faults along with parameter uncertainties, based on which the adaptive FTC problem for scalar hyperbolic PDE system is effectively addressed.

The remainder of this article is as follows: In Section 2, the output-feedback boundary adaptive FTC problem is formulated for scalar hyperbolic PDE. In Section 3, the parameter updating laws are developed and the adaptive FTC scheme is proposed. In Section 4, the stability of the closed-loop system is analyzed. The simulation studies are presented to validate the results in Section 5. In the end, the conclusion of this article is given in Section 6.

Notations: For a nonlinear function $f(t,x)$, let $f_x(t,x)$ and $f_t(t,x)$ represent $\frac{\partial f(t,x)}{\partial x}$ and $\frac{\partial f(t,x)}{\partial t}$, respectively, The norm of $f(t,x)$ is denoted by $||f(t,x)|| = \left(\int_0^1 f^2(t,x)dx\right)^{\frac{1}{2}}$. $f(*) \in C(\Omega)$ denotes that $f(*)$ is continuous on Ω and $f(*) \in C^1(\Omega)$ denotes that $f(*)$ is derivative continuous on Ω. For a nonlinear function $F(t)$ defined on $t > 0$, $F(t) \in L_1$ represents that $F(t)$ is integrable for $t > 0$, $F(t) \in L_2$ represents that $F(t)$ is square integrable for $t > 0$, $F(t) \in L_\infty$ represents that $F(t)$ is bounded for $t > 0$.

2 | PROBLEM FORMULATION

Consider the faulty hyperbolic PDE system, which is described by

$$\begin{cases} z_t(t,x) = z_x(t,x) + h(x)z(t,0) + \int_0^x f(x,y)z(t,y)dy, & x \in [0,1], \\ z(t,1) = u^f(t), & y(t) = z(t,0), \end{cases} \tag{1}$$

where $h(x) \in C([0,1])$ and $f(x,y) \in C([0,1] \times [0,1])$ are unknown functions, and $z(t,x)$ represents the system state. The output signal of the faulty actuator is denoted by $u^f(t)$ and the sensor measurement signal (system output) is denoted by $y(t)$. The combined multiplicative and additive actuator faults in Reference 7 are considered, which can be modeled as follows:

$$u^f(t) = (1 - \rho_u)u(t) + \varepsilon = \Theta u(t) + \varepsilon, \tag{2}$$

where ρ_u denotes the unknown actuator fault factor, $\Theta = (1 - \rho_u)$ denotes the unknown effective rate of actuator, and ε denotes the unknown deviation fault value. The signals $u(t)$ and $u^f(t)$ denote the input and output of actuator, respectively.

Before proceeding further, the following assumption is first given:

Assumption 1. The unknown effective rate Θ is bounded by

$$0 < \Theta_m \le \Theta \le 1, \tag{3}$$

where Θ_m is a known positive constant.

For large positive functions $h(x)$ and $f(x,y)$, the target system (1) will be unstable with $u^f(t) = 0$ (see Reference 28). Therefore, the objective of this article is to achieve $\lim_{t\to\infty} z(t,x) = 0$ for any $x \in [0,1]$. And only the sensor measurement $y(t)$ and the actuator input $u(t)$ are available in our adaptive FTC design.

For ease of analysis, the original PDE system (1) should be further simplified. With the following transformation

$$v(t,x) = z(t,x) - \int_0^x p(x,s)z(t,s)ds, \tag{4}$$

where $p(x,s)$ satisfies

$$p_x(x,s) + p_s(x,s) = \int_s^x p(x,\xi)f(\xi,s)d\xi - f(x,s), \quad p(1,s) = 0. \tag{5}$$

The original system (1) can be converted into the following observer canonical form (proposed in Reference 37)

$$\begin{cases} v_t(t,x) = v_x(t,x) + g(x)v(t,0), \\ v(t,1) = u^f(t), \;\; y(t) = v(t,0), \end{cases} \tag{6}$$

where $g(x)$ is defined by

$$g(x) = p(x,0) + h(x) - \int_0^x p(x,s)h(s)ds. \tag{7}$$

The inverse transformation of (4) can be described as follows:

$$z(t,x) = v(t,x) + \int_0^x l(x,s)v(t,s)ds. \tag{8}$$

For the existence, uniqueness and boundness of $p(x,s)$ and $l(x,s)$, please refer to Reference 37.

It is obtained from the transformation (4) that $v(t,0) = z(t,0)$ and the zero equilibrium of these two systems are equivalent. As a consequence, for the output-feedback adaptive FTC problem, the observer canonical form (6) is equivalent to the target system (1).

3 | CONTROL DESIGN SCHEME

3.1 | Observer design

To make full use of $u(t)$ and $y(t)$, two filters are constructed as follows:

$$\begin{cases} \alpha_t(t,x) = \alpha_x(t,x), & \alpha(t,1) = u(t), \\ \alpha(0,x) = \alpha_0(x), & x \in [0,1], \end{cases} \tag{9}$$

$$\begin{cases} \beta_t(t,x) = \beta_x(t,x), & \beta(t,1) = y(t), \\ \beta(0,x) = \beta_0(x), & x \in [0,1], \end{cases} \tag{10}$$

where α_0 and β_0 are the arbitrary initial conditions of the two filters with $\alpha_0, \beta_0 \in C^1[0,1]$.

It should be noted that the solutions of the above two PDEs are described as follows:

$$\begin{cases} \alpha(t,x) = u(t+x-1),\ \beta(t,x) = y(t+x-1), & t+x-1 > 0, \\ \alpha(t,x) = \alpha_0(t+x),\ \beta(t,x) = \beta_0(t+x), & t+x-1 \le 0, \end{cases} \tag{11}$$

which implies that $\alpha(t,x)$ and $\beta(t,x)$ are the delay signals of $u(t)$ and $y(t)$, respectively. For ease of description, the variable t will be omitted for some equations in the remainder of this article.

Based on the filters (10) and (11), the following error variable is defined

$$e(x) = v(x) - \Theta\alpha(x) - \int_x^1 g(s)\beta(1+x-s)ds - \varepsilon. \tag{12}$$

In view of (6), (9), (10), and (12), one has

$$e_t(t,x) = e_x(t,x), \quad e(t,1) = 0, \tag{13}$$

which indicates that $e(t,x) \in L_2 \cap L_\infty$ and $e(t,x) = 0$ for $t > 1$. Consequently, the system state $v(t,x)$ can be estimated by the following equation, if Θ, ε and $g(x)$ are known

$$\hat{v}_o(x) = \Theta\alpha(x) + \int_x^1 g(s)\beta(1+x-s)ds + \varepsilon. \tag{14}$$

Then, the following alternative observer is constructed

$$\hat{v}(x) = n(x) + \int_x^1 \hat{g}(s)\beta(1+x-s)ds, \tag{15}$$

where the function $n(t,x)$ is defined by

$$n(x) = \hat{\Theta}\alpha(x) + \hat{\varepsilon}, \tag{16}$$

in which $\hat{\Theta}$, $\hat{\varepsilon}$, and $\hat{g}$ are the estimations of Θ, ε, and g, respectively, and their parameter updating laws will be given in the following section.

Moreover, the dynamics of $n(t,x)$ and $\hat{v}(t,x)$ are given as follows:

$$\begin{cases} n_t(x) = n_x(x) + \frac{\hat{\Theta}_t}{\hat{\Theta}}(n(x) - \hat{\varepsilon}) + \hat{\varepsilon}_t, \\ n(1) = \hat{\Theta}u + \hat{\varepsilon}, \end{cases} \tag{17}$$

$$\begin{cases} \hat{v}_t(x) = \hat{v}_x(x) + \hat{g}(x)v(0) + \frac{\hat{\Theta}_t}{\hat{\Theta}}(n(x) - \hat{\varepsilon}) + \int_x^1 \hat{g}_t(s)\beta(1+x-s)ds + \hat{\varepsilon}_t, \\ \hat{v}(1) = \hat{\Theta}u + \hat{\varepsilon}. \end{cases} \tag{18}$$

3.2 | Parameters updating laws

Define the following error variable

$$\begin{aligned}\hat{e}(x) &= v(x) - \hat{v}(x) = v(x) - \hat{\Theta}\alpha(x) - \int_x^1 \hat{g}(s)\beta(1+x-s)ds - \hat{\varepsilon}\\ &= e(x) + \tilde{\Theta}\alpha(x) + \int_x^1 \tilde{g}(s)\beta(1+x-s)ds + \tilde{\varepsilon},\end{aligned} \tag{19}$$

where $\tilde{\Theta}(t)$, $\tilde{\varepsilon}(t)$, and $\tilde{g}(t,x)$ are defined as follows:

$$\tilde{\Theta} = \Theta - \hat{\Theta}, \quad \tilde{\varepsilon} = \varepsilon - \hat{\varepsilon}, \quad \tilde{g}(x) = g(x) - \hat{g}(x). \tag{20}$$

Setting $x = 0$ in Equation (19), one has

$$\begin{aligned}\hat{e}(0) &= v(0) - \hat{\Theta}\alpha(0) - \int_0^1 \hat{g}(s)\beta(1-s)ds - \hat{\varepsilon}\\ &= e(0) + \tilde{\Theta}\alpha(0) + \int_0^1 \tilde{g}(s)\beta(1-s)ds + \tilde{\varepsilon}.\end{aligned} \tag{21}$$

The above equation is chosen as the parametric model to identify actuator faults as well as the unknown coefficient $g(x)$, since all the involved signals are available. Based on the parametric model (21), parameter updating laws of gradient type are designed as follows:

$$\begin{aligned}&\hat{\Theta}_t = \mathrm{Proj}_{[\Theta_m,1]}\left\{\tau, \hat{\Theta}\right\}, \quad \tau = \frac{\gamma_1 \hat{e}(0)\alpha(0)}{1+n^2(0)+||\beta(x)||^2}, \quad \hat{\Theta}(0) = 1,\\ &\hat{\varepsilon}_t = \frac{\gamma_2 \hat{e}(0)}{1+n^2(0)+||\beta(x)||^2}, \quad \hat{\varepsilon}(0) = 0, \quad \hat{g}_t(x) = \frac{\gamma_3(x)\hat{e}(0)\beta(1-x)}{1+n^2(0)+||\beta(x)||^2}, \quad \hat{g}(0,x) = 0,\end{aligned} \tag{22}$$

where γ_1, γ_2, and γ_3 are positive parameters, and the projection operator is defined as follows:

$$\mathrm{Proj}_{[\Theta_m,1]}\left\{\tau, \hat{\Theta}\right\} = \begin{cases} 0, & \hat{\Theta} \le \Theta_m, \ \tau < 0,\\ 0, & \hat{\Theta} \ge 1, \quad \tau > 0,\\ \tau, & \text{else}.\end{cases} \tag{23}$$

It follows from the properties of the projection operator[37] that

$$\hat{\Theta} \in [\Theta_m, 1], \quad \hat{\Theta}_t^2 \le \tau^2, \quad -\tilde{\Theta}\hat{\Theta} \le -\tau\tilde{\Theta}. \tag{24}$$

Then, we have the following lemma.

Lemma 1. *With the parameter updating laws (22), the following properties hold*

$$\begin{aligned}&\tilde{\Theta}, \tilde{\varepsilon}, ||\tilde{g}(x)|| \in L_\infty,\\ &\left|\hat{\Theta}_t\right|, |\hat{\varepsilon}_t|, ||\hat{g}_t(x)|| \in L_2 \cap L_\infty,\\ &\frac{\hat{e}(0)}{\sqrt{1+n^2(0)+||\beta(x)||^2}} \in L_2 \cap L_\infty.\end{aligned} \tag{25}$$

Proof. Inspired by Bernard and Krstic,[37] we select the following Lyapunov candidate

$$V_1 = \frac{1}{2}||e(x)||^2 + \frac{\tilde{\Theta}^2}{2\gamma_1} + \frac{\tilde{\varepsilon}^2}{2\gamma_2} + \int_0^1 \frac{\tilde{g}^2(s)ds}{2\gamma_3(x)}. \tag{26}$$

Then, we have

$$\begin{aligned}\dot{V}_1 &= -e^2(0) - \frac{\tilde{\Theta}\hat{\Theta}_t}{\gamma_1} - \frac{\tilde{\varepsilon}(t)\hat{\varepsilon}_t(t)}{\gamma_2} - \int_0^1 \frac{\tilde{g}(s)\hat{g}(s)}{\gamma_3(x)} \\ &\le -e^2(0) + \frac{\hat{e}(0)e(0) - \hat{e}^2(0)}{1 + n^2(0) + ||\beta(x)||^2} \\ &\le -\frac{\hat{e}^2(0)}{2(1 + n^2(0) + ||\beta(x)||^2)},\end{aligned} \tag{27}$$

which yields

$$\tilde{\Theta}, \tilde{\varepsilon}, ||\tilde{g}(x)|| \in L_\infty, \quad \frac{\hat{e}(0)}{\sqrt{1 + n^2(0) + \beta^2(x)}} \in L_2. \tag{28}$$

Furthermore, in view of (15)–(19), it is obtained that

$$\frac{\alpha^2(0)}{1 + n^2(0) + ||\beta(x)||^2} \le \frac{2\left(\hat{n}^2(0) + \hat{\varepsilon}^2\right)}{\left(1 + n^2(0) + ||\beta(x)||^2\right)\hat{\Theta}^2} < \infty, \tag{29}$$

$$\frac{\hat{e}^2(0)}{1 + n^2(0) + ||\beta(x)||^2} \le \frac{2\left(e^2(0) + \tilde{\Theta}^2\alpha^2(0) + \tilde{\varepsilon}^2\right)}{1 + n^2(0) + ||\beta(x)||^2} < \infty. \tag{30}$$

Consequently, combined with (28)–(30), the property (25) is proved. ■

It follows from the properties $\tilde{\Theta}(t), \tilde{\varepsilon}(t) \in L_\infty$ that $\hat{\Theta}(t)$ and $\hat{\varepsilon}(t)$ are bounded.

3.3 | Backstepping control design

In this subsection, the backstepping method is utilized to design the adaptive FTC scheme. Motivated by Xu and Liu,[34] we define $\hat{k}(t, x)$ which satisfies

$$\hat{k}(x) = \int_0^x \hat{k}(x - s)\hat{g}(s)ds - \hat{g}(x). \tag{31}$$

Then, the transformation is described by

$$\hat{w}(x) = T_1[\hat{v}](x) \overset{\Delta}{=} \hat{v}(x) - \int_0^x \hat{k}(x - s)\hat{v}(s)ds \tag{32}$$

and its inverse transformation is described as follows:

$$\hat{v}(x) = T_2[\hat{w}](x) \overset{\Delta}{=} \hat{w}(x) - \int_0^x \hat{w}(s)\hat{g}(x - s)ds. \tag{33}$$

Lemma 2. *If $||\tilde{g}(t, x)|| \in L_\infty$, then the existence and uniqueness of $\hat{k}(t, x)$, which is the solution of (31), are guaranteed, and $||\hat{k}(t, x)||$ is uniformly bounded.*

Proof. It follows from $||\tilde{g}(t, x)|| \in L_\infty$ that

$$\int_0^1 \tilde{g}(x)dx \in L_\infty. \tag{34}$$

Furthermore, one has

$$\int_0^1 \hat{g}^2(x)dx = \int_0^1 \left(\tilde{g}^2(x) + g^2(x) - 2g(x)\tilde{g}(x)\right) dx \in L_\infty. \tag{35}$$

We assume that M_g is an upper bound of $||\hat{g}(t,x)||$.

Then, we define the following sequence

$$\hat{k}_0(t,x) = -\hat{g}(t,x), \quad \hat{k}_{N+1}(t,x) = \int_0^x \hat{k}_N(x-s)\hat{g}(t,s)ds - \hat{g}(t,x) \tag{36}$$

and their differences

$$\Delta\hat{k}_0(t,x) = -\hat{g}(t,x), \quad \Delta\hat{k}_{N+1}(t,x) = \hat{k}_{N+1}(t,x) - \hat{k}_N(t,x) = \int_0^x \Delta\hat{k}_N(x-s)\hat{g}(t,s)ds. \tag{37}$$

When $N = 1$, one has

$$|\Delta\hat{k}_1(t,x)| = \left|\int_0^x -\hat{g}(t,x-s)\hat{g}(t,s)ds\right| \le M_g^2. \tag{38}$$

We assume that for $N \ge 1$

$$|\Delta\hat{k}_N(t,x)| \le \frac{M_g^{N+1}x^{N-1}}{(N-1)!}. \tag{39}$$

Then it can be deduced that

$$\begin{aligned} |\Delta\hat{k}_{N+1}(t,x)| &= \left|\int_0^x \frac{M_g^{N+1}(x-s)^{N-1}}{(N-1)!} g(t,s)ds\right| \\ &\le \frac{M_g^{N+2}}{(N-1)!}\left(\int_0^x (x-s)^{2(N-1)}ds\right)^{\frac{1}{2}} \le \frac{M_g^{N+2}x^N}{N!}. \end{aligned} \tag{40}$$

Consequently, by induction, one obtains that for $N \ge 1$

$$|\Delta\hat{k}_N(t,x)| \le \frac{M_g^{N+1}x^{N-1}}{(N-1)!} \le \frac{M_g^{N+1}}{(N-1)!}, \tag{41}$$

which implies that the series

$$\hat{k}(t,x) = \lim_{N\to\infty} \hat{k}_N(t,x) = -\hat{g}(t,x) + \sum_{N=1}^{\infty} \Delta\hat{k}_N(t,x) \tag{42}$$

uniformly converges to the integral equation (31) in $x \in [0,1]$ and

$$|\hat{k}(t,x)| \le |\hat{g}(t,x)| + M_g e^{M_g}, \quad ||\hat{k}(t,x)|| \in L_\infty. \tag{43}$$

The uniqueness of $\hat{k}(t,x)$ can also be proved, which is similar to Section 6.1 in Reference 37. ∎

Lemma 3. *The dynamics of $\hat{w}(x)$ can be described as follows:*

$$\begin{cases} \hat{w}_t(x) = \hat{w}_x(x) + \frac{\hat{\Theta}_t}{\hat{\Theta}} T_1(n(x) - \hat{\varepsilon}) + T_1(\hat{\varepsilon}_t(t)) - \hat{k}(t,x)\hat{e}(t,0) \\ \qquad + T_1\left(\int_x^1 \hat{g}_t(s)\beta(1+x-s)ds\right) + \int_0^x \hat{w}(x)T_1\left(\hat{g}_t(x-s)\right)ds, \\ \hat{w}(1) = \hat{\Theta}u + \hat{\varepsilon} - \int_0^1 \hat{k}(1-y)\hat{v}(y)dy. \end{cases} \tag{44}$$

Proof. With the dynamics of $\hat{v}(x,t)$, it can be obtained that

$$\hat{w}_x(x) = \hat{v}_x(x) - \hat{k}(0)\hat{v}(x) - \int_0^x \hat{k}_x(x-s)\hat{v}(s)ds, \tag{45}$$

$$\begin{aligned}\hat{w}_t(x) = {} & T_1(\hat{v}_x(x) + \hat{g}(x)v(0)) + \frac{\hat{\Theta}_t}{\hat{\Theta}} T_1(n(x) - \hat{\varepsilon}) + T_1(\hat{\varepsilon}_t) \\ & + T_1\left(\int_x^1 \hat{g}_t(s)\beta(1+x-s)ds\right) - T_1\left(\int_0^x \hat{k}_t(x-s)\hat{v}(s)ds\right).\end{aligned} \tag{46}$$

With the technique of integration by parts, one obtains

$$T_1(\hat{v}_x(x) + \hat{g}(x)v(0)) = \hat{v}_x(x) - \hat{k}(x)\hat{e}(0) - \hat{k}(0)\hat{v}(x) - \int_0^x \hat{k}_x(x-s)\hat{v}(s)ds. \tag{47}$$

Moreover, it is proved that

$$\int_0^x \hat{k}_t(x-s)\hat{v}(s)ds = \int_0^x \hat{k}_t(s)T_2(\hat{w}(x-s))ds = \int_0^x \hat{w}(s)T_2(\hat{k}_t(x-s))ds. \tag{48}$$

Therefore, it can be deduced from (31) that

$$T_2(\hat{k}_t(x-s)) = -T_1(\hat{g}_t(x-s)). \tag{49}$$

Eventually, the dynamics (44) can be derived from (45)–(48). ■

To achieve $\hat{w}(1) = 0$ in (44), the following backstepping control law is designed

$$u = \frac{1}{\hat{\Theta}}\left(\int_0^1 \hat{k}(1-y)\hat{v}(y)dy - \hat{\varepsilon}\right). \tag{50}$$

Then, the above analysis can be summarized in the following theorem.

Theorem 1. *The system (1) can be stabilized by the control law (50) with the parameter updating laws (22) and the observer (15) in the following sense*

$$\lim_{t\to\infty} z(t,x) = 0, \quad \forall x \in [0,1] \tag{51}$$

and the boundness of all the closed-loop system signals is guaranteed.

Proof. The detailed proof will be presented in Section 4. ■

4 | STABILITY ANALYSIS

The stability of the closed-loop system will be analyzed in this section. Before proceeding further, two lemmas are presented as follows:

Lemma 4. *Let $V(t) \in C^1([0,+\infty))$, $l_i(t) \in L_1$, $i = 1,2,3$ and $b(t)$ be the non-negative functions defined on $[0,+\infty)$. If the following differential inequality holds*

$$\dot{V} \le -a_1 V + l_1 V + l_2 + (l_3 - a_2)\, b, \quad V(0) \ge 0 \tag{52}$$

in which a_1 and a_2 are two positive constants, then $V(t) \in L_1 \cap L_\infty$.

Proof. It follows from $l_3(t) \in L_1$ that

$$\exists t_0 > 0 \quad s.t \quad \int_{t_0}^{\infty} (l_3(s) - a_2)\, b(s) ds < 0. \tag{53}$$

Then, we define a function $W(t)$ by the following ODE

$$\dot{W} = -a_1 W + l_1 W + l_2 + (l_3 - a_2)\, W, \quad W(t_0) = V(t_0), \tag{54}$$

which yields

$$W(t) = V(t_0)\mathrm{e}^{\int_{t_0}^{t}(-a_1+l_1(s))ds} + \int_{t_0}^{t} \mathrm{e}^{\int_{\tau}^{t}(-a_1+l_1(s))ds} (l_2(\tau) + (l_3(\tau) - a_2)\, b(\tau))\, d\tau. \tag{55}$$

It follows from the comparison principle that $V(t) \le W(t)$ when $t \ge t_0$. Therefore, for $t \ge t_0$, one has

$$\begin{aligned} V(t) &\le V(t_0)\mathrm{e}^{\int_{t_0}^{t}(-a_1+l_1(s))ds} + \int_{t_0}^{t} \mathrm{e}^{\int_{\tau}^{t}(-a_1+l_1(s))ds} (l_2(\tau) + (l_3(\tau) - a_2)\, b(t))\, d\tau \\ &\le \left(V(t_0)\mathrm{e}^{-a_1(t-t_0)} + \int_{t_0}^{t} \mathrm{e}^{-a_1(t-t_0-\tau)} l_2(\tau) d\tau \right) \mathrm{e}^{\int_0^{\infty} l_1(s)ds} < +\infty. \end{aligned} \tag{56}$$

Moreover, it is obvious that $V(t)$ is bounded in the interval $[0, t_0]$, since $V(t)$ is continuous. As a consequence, it is proved that $V(t) \in L_\infty$.

Furthermore, integrating (56) over $[t_0, t]$, one has

$$\begin{aligned} \int_{t_0}^{t} V(s) ds &\le \left(\frac{V(t_0)}{a_1} + \mathrm{e}^{a_1 t_0} \int_0^t \int_0^{\tau} \mathrm{e}^{-a_1(\tau - s)} l_2(s) ds d\tau \right) \mathrm{e}^{\int_0^{\infty} l_1(s)ds} \\ &\le \left(\frac{V(t_0)}{a_1} + \mathrm{e}^{a_1 t_0} \int_0^t \int_s^{t} \mathrm{e}^{-a_1(\tau - s)} l_2(s) d\tau ds \right) \mathrm{e}^{\int_0^{\infty} l_1(s)ds} \\ &\le \left(V(t_0) - \mathrm{e}^{a_1 t_0} \int_0^t \left(1 + \mathrm{e}^{-a_1(t-s)}\right) l_2(s) ds \right) \frac{\mathrm{e}^{\int_0^{\infty} l_1(s)ds}}{a_1} \\ &< +\infty. \end{aligned} \tag{57}$$

Then, it follows from (57) that $V(t) \in L_1$. ∎

Lemma 5. *For two functions $a(x)$ and $b(x)$, the following inequality holds*

$$\int_0^1 a(x)b(x)dx \le c||a(x)||^2 + d||b(x)||^2, \tag{58}$$

where c and d are two arbitrary positive constants satisfying $cd \ge \frac{1}{2}$.

Proof. This lemma can be proved by the integral form of Cauchy inequality, which is omitted here. ∎

It follows from (4) and (8) that

$$\lim_{t\to\infty} z(t,x) = 0 \Leftrightarrow \lim_{t\to\infty} v(t,x) = 0. \tag{59}$$

Similarly, it follows from (32) and (33) that

$$\lim_{t\to\infty} \hat{w}(t,x) = 0 \Leftrightarrow \lim_{t\to\infty} \hat{v}(t,x) = 0. \tag{60}$$

4.1 Pointwise boundness

In this subsection, the pointwise boundness of all the signals involved in the control scheme will be proved. The following Lyapunov function candidates are first given

$$V_2=\int_0^1(1+x)\hat{w}^2(x)dx,\quad V_3=\int_0^1(1+x)n^2(x)dx,\quad V_4=\int_0^1(1+x)\beta^2(x)dx. \tag{61}$$

It follows from the dynamics of $\hat{w}(t,x)$ and Lemma 5 that

$$\begin{aligned}\dot{V}_2=&\int_0^1 2(1+x)\hat{w}(x)\hat{w}_x(x)dx+\frac{\hat{\Theta}_t}{\hat{\Theta}}\int_0^1 2(1+x)\hat{w}(x)T_1[n(x)-\hat{\varepsilon}]dx\\&+\int_0^1 2(1+x)\hat{w}(x)\left(\varepsilon_t-\hat{k}(x)\hat{e}(0)+T_1\left[\int_x^1\hat{g}_t(s)\beta(s)ds\right]\right)dx\\&+\int_0^1\int_0^x 2(1+x)\hat{w}(x)\hat{w}(s)T_1[\hat{g}_t(x-s)]dsdx\\\le&-\hat{w}^2(0)-||\hat{w}(x)||^2+d_1\hat{\Theta}_t^2||n(x)||^2+c_1||\hat{w}(x)||^2+d_2\hat{\Theta}_t^2\\&+c_2||\hat{w}(x)||^2+d_3\hat{\varepsilon}_t^2+c_3||\hat{w}(x)||^2+d_4\hat{e}^2(0)+c_4||\hat{w}(x)||^2\\&+d_5||\hat{g}_t(x)||^2||\beta(x)||^2+c_5||\hat{w}(x)||^2+d_6||\hat{g}_t(x)||^2+c_6||\hat{w}(x)||^2\\\le&-\hat{w}^2(0)-\left(1-\sum_{i=1}^6c_i\right)||\hat{w}(x)||^2+d_1\hat{\Theta}_t^2||n(x)||^2+d_2\hat{\Theta}_t^2+d_3\hat{\varepsilon}_t^2\\&+d_4\hat{e}^2(0)+d_5||\hat{g}_t(x)||^2||\beta(x)||^2+d_6||\hat{g}_t(x)||^2.\end{aligned} \tag{62}$$

Similarly, it follows from the dynamics of $n(t,x)$, the control law (50) and Lemma 5 that

$$\begin{aligned}\dot{V}_3=&\int_0^1 2(1+x)n(x)n_x(x)dx+\int_0^1 2(1+x)n(x)\left(\frac{\hat{\Theta}_t}{\hat{\Theta}}(n(x)-\hat{\varepsilon})+\hat{\varepsilon}_t\right)dx\\\le&\,2\int_0^1\hat{k}(1-y)\hat{v}(y)dy-n^2(0)-(1-c_7-c_8)||n(x)||^2+d_7\hat{\Theta}_t^2+d_8\hat{\varepsilon}_t^2\\\le&\,m_1||\hat{w}(x)||^2-n^2(0)-(1-c_7-c_8)\,||n(x)||^2+d_7\hat{\Theta}_t^2+d_8\hat{\varepsilon}_t^2,\end{aligned} \tag{63}$$

where m_1 is an appropriate positive constant. For (62) and (63), c_i and d_i represent two arbitrary positive constants which satisfy $c_id_i\ge M_i,\ i=1,\dots,8$, with $M_i,\ i=1,\dots,8$ being the appropriate positive constants and make (62) and (63) truthful. The boundness of $\hat{\Theta}(t)$, $\hat{\varepsilon}(t)$ and $||\hat{k}(t,x)||$ guarantee the existence of $M_i,\ i=1,\dots,8$. For the ease of the following analysis, the values of $c_i, i=1,\dots,8$ are set as $c_i=\frac{1}{12},\ i=1,\dots,6$ and $c_7=c_8=\frac{1}{4}$.

In view of (10) and (19), one has

$$\dot{V}_4\le 2v^2(0)-\beta^2(0)-||\beta(x)||^2\le 4\hat{e}^2(0)+4\hat{w}^2(0)-\beta^2(0)-||\beta(x)||^2. \tag{64}$$

The following Lyapunov candidate is given

$$V_5=4V_2+\frac{V_3}{m_1}+V_4. \tag{65}$$

Based on (62)–(65) and Lemma 1, it is proved that

$$\dot{V}_5\le -m_2V_5+m_3l_1V_5+m_4l_2+\left(m_5l_3-\frac{1}{m_1}\right)n^2(0), \tag{66}$$

where $m_i,\ i=2,\dots,5$ are appropriate positive constants and $l_i(t),\ i=1,2,3$ are described by

$$l_3=\frac{\hat{e}^2(0)}{1+n^2(0)+||\beta(x)||^2},\quad l_1=\hat{\Theta}_t^2+||\hat{g}_t(x)||^2+l_3,\quad l_2=l_1+\hat{\varepsilon}_t^2, \tag{67}$$

which indicate that $l_1,l_2,l_3\in L_1\cap L_\infty$. Consequently, combined with Lemma 4, it can be deduced that $V_5(t)\in L_1\cap L_\infty$.

Furthermore, combined with (15) and (65), one has

$$||\hat{v}(x)|| \in L_2 \cap L_\infty, \quad ||n(x)|| \in L_2 \cap L_\infty, \quad ||\beta(x)|| \in L_2 \cap L_\infty. \tag{68}$$

The pointwise boundness of $u(t)$ and $\alpha(t,x)$ follows from (10), (50), and (68). With (13), (15), and (16), it can be deduced that $n(t,x)$, $\hat{v}(t,x)$ and $v(t,x)$ are pointwise bounded. As a consequence, it is obvious that the input signal $u(t)$ and the output signal $y(t)$ are both bounded. The pointwise boundness of $\beta(t,x)$ and $z(t,x)$ can also be deduced from the above analysis.

4.2 | Pointwise convergence

In view of (11), (16), (21), (68) and the boundness of $n(t,0)$, it can be obtained that $\hat{e}^2(t,0) \in L_1$. Additionally, based on (21) and the boundness of all the variables, the boundness of $\hat{e}_t(t,0)$ can be proved. Thus, it follows from Barbalat's lemma that $\hat{e}^2(t,0) \to 0$.

Furthermore, in view of (22) and the boundness of $\alpha(t,0)$, one has

$$\lim_{t\to\infty} \hat{\Theta}_t = 0, \quad \lim_{t\to\infty} \hat{\varepsilon}_t = 0, \tag{69}$$

which indicates that $\hat{\Theta}(t)$ and $\hat{\varepsilon}(t)$ will converge to two constants.

It follows from (66) and $V_5(t) \in L_\infty$ that $\dot{V}_5(t)$ is bounded. Therefore, based on Barbalat's lemma, it can be obtained that $V_5(t) \to 0$, which implies

$$\lim_{t\to\infty} ||\hat{v}(x)|| = 0, \quad \lim_{t\to\infty} ||\beta(x)|| = 0, \quad \lim_{t\to\infty} ||n(x)|| = 0. \tag{70}$$

By using (11), (16), and (50), one has

$$\begin{aligned} n(x) &= \hat{\Theta}\alpha(x) + \hat{\varepsilon} \\ &= \frac{\hat{\Theta}(t)}{\hat{\Theta}(t+x-1)} \left(\int_0^1 \hat{k}(t, 1-y)\hat{v}(t+x-1, y)dy - \hat{\varepsilon}(t+x-1) \right) + \hat{\varepsilon}(t). \end{aligned} \tag{71}$$

Then, by combining with (15), (69), and (70), one has

$$\lim_{t\to\infty} n(x) = 0, \quad \lim_{t\to\infty} \hat{v}(x) = 0, \quad \forall x \in [0,1]. \tag{72}$$

Furthermore, it can be deduced that

$$\begin{aligned} \lim_{t\to\infty} v(x) &= \lim_{t\to\infty} \left(e(x) + \hat{v}(x) + \tilde{\Theta}\alpha(x) + \tilde{\varepsilon} + \int_x^1 \tilde{g}(s)\beta(1+x-s)ds \right) \\ &= \lim_{t\to\infty} \left(\tilde{\Theta}\alpha(x) + \tilde{\varepsilon}\right) = \lim_{t\to\infty} \left(\hat{e}(0) - e(0) + \frac{\tilde{\Theta}}{\hat{\Theta}}(n(x) - n(0)) \right) = 0. \end{aligned} \tag{73}$$

Therefore, it can be obtained that

$$\lim_{t\to\infty} u(t) = -\frac{\varepsilon}{\Theta}. \tag{74}$$

Finally, it follows from the inverse transformation (8) that

$$\lim_{t\to\infty} z(t,x) = 0, \quad \forall x \in [0,1]. \tag{75}$$

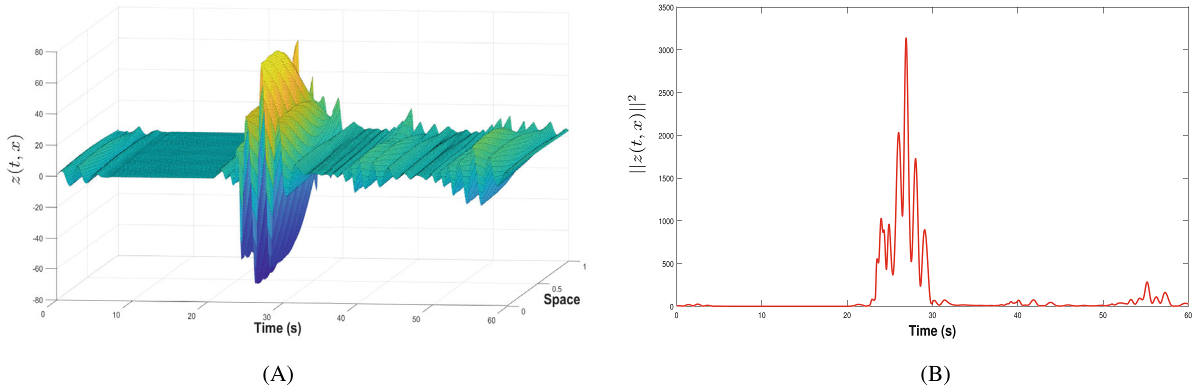

FIGURE 1 Trajectories of the system states (A) $z(t, x)$ and (B) $||z(t, x)||^2$ with adaptive control scheme

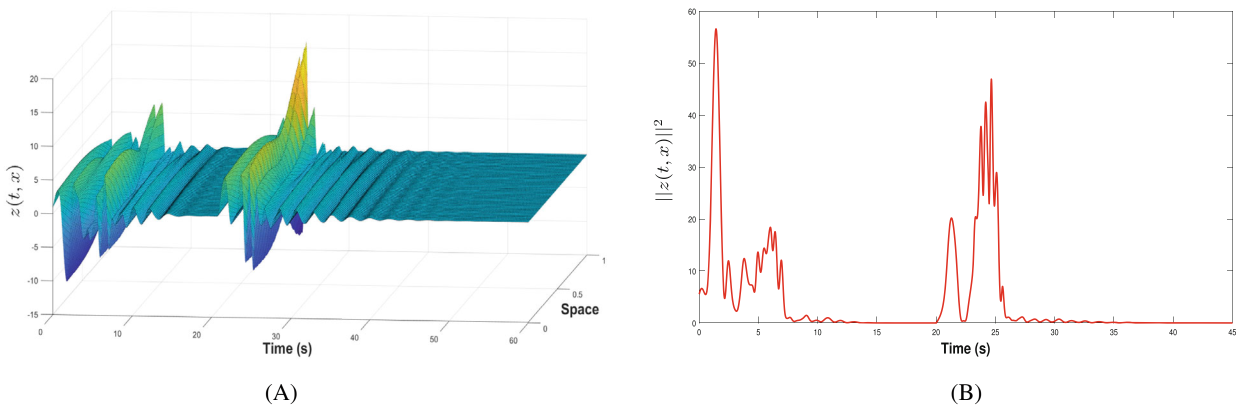

FIGURE 2 Trajectories of the system states (A) $z(t, x)$ and (B) $||z(t, x)||^2$ (adaptive FTC control scheme)

5 | SIMULATION STUDIES

In this section, the following numerical example, which is referred to as the Korteweg–de Vries-like equations,[28] is utilized to validate the effectiveness of the proposed output-feedback boundary adaptive FTC scheme

$$\begin{cases} z_t(t,x) = z_x(t,x) - 4z(t,0)\sinh(x) + 4\int_0^x z(t,y)\cosh(x-y)dy, \\ z(t,1) = u^f(t), \quad y(t) = z(t,0), \quad z(0,x) = 1 + 2\sin(\pi x), \end{cases} \tag{76}$$

and the explicit forward Euler method[46] is utilized for the simulation of PDE (76).

It is shown in Reference 37 that the system (76) will be unstable if $u^f(t) = 0$. In simulation studies, the actuator output signal $u^f(t)$ is selected as follows:

$$\begin{cases} u^f(t) = u(t), & 0 < t < 20, \\ u^f(t) = 0.5u(t) + 2, & t \geq 20, \end{cases} \tag{77}$$

which indicates that the combined multiplicative and additive actuator faults occur at $t = 20$.

5.1 | Adaptive control scheme

To highlight the effectiveness of the proposed output-feedback boundary adaptive FTC control scheme, the previous output-feedback boundary adaptive control scheme,[37] which can only stabilize the target system with no actuator faults,

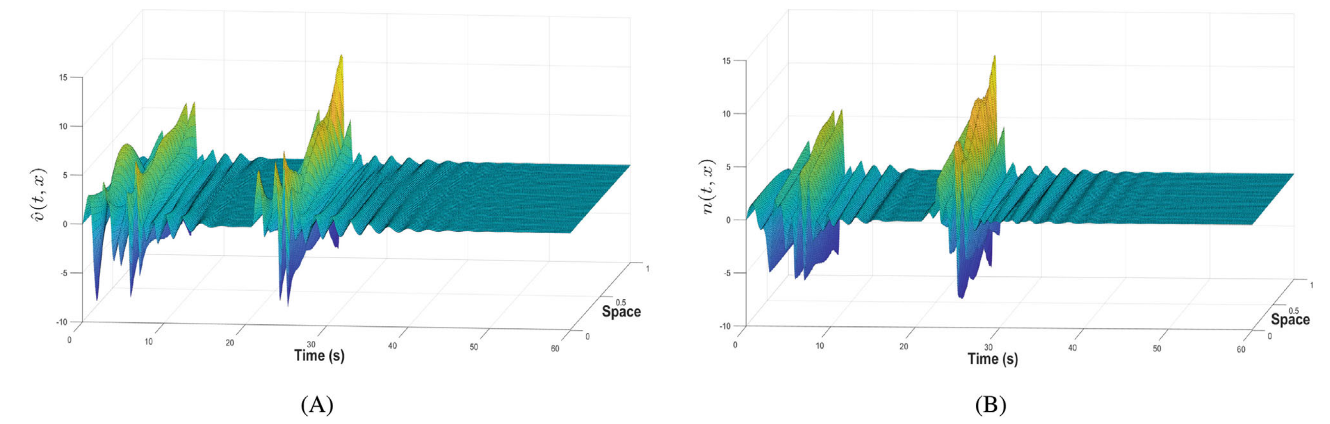

FIGURE 3 Trajectories of observer states (A) $\hat{v}(t,x)$ and (B) $n(t,x)$

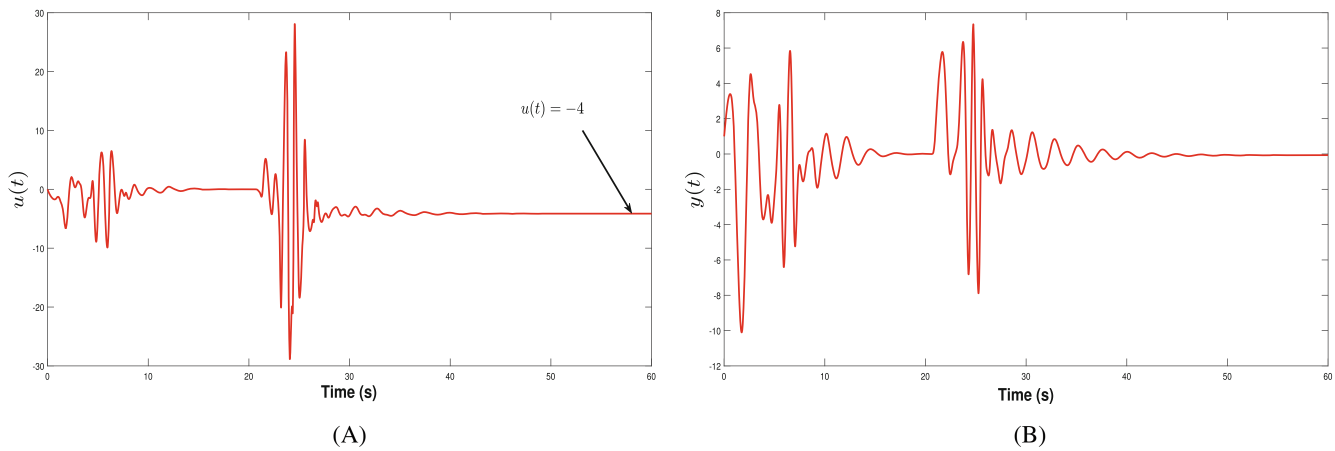

FIGURE 4 Trajectories of (A) the control signal $u^f(t)$ and (B) the output signal $y(t)$

is utilized for comparison in simulations. Figure 1 shows that when actuator works normally, the adaptive control scheme can stabilize system (76), when $t \geq 20$ the system state $z(t,x)$ is oscillating constantly due to actuator faults. Obviously, it can be concluded from the above results that the adaptive control scheme proposed in Reference 37 cannot accommodate the actuator faults (77).

5.2 | Adaptive fault-tolerant control scheme

The simulation results of the proposed output-feedback boundary adaptive FTC control scheme are presented in Figures 2–6. The gains of parameter updating laws are chosen as $\gamma_1 = 3$, $\gamma_2 = 5$, and $\gamma_3(x) = 4$. Figure 2 depicts the trajectories of $z(t,x)$ and $||z(t,x)||^2$. It can be concluded from Figure 2 that when actuator operates normally the adaptive FTC law can stabilize the system state $z(t,x), \forall x \in [0,1]$. When $t \geq 20$ the system state $z(t,x), \forall x \in [0,1]$ still converges to zero after an oscillation caused by actuator faults. Figure 3 gives the trajectories of $\hat{v}(t,x)$ and $n(t,x)$, which both converge to zero when $t \geq 20$. The trajectories of $u(t)$ and $y(t)$ are depicted in Figure 4. It is shown from Figure 4A that when actuator operates normally, the control signal $u(t)$ will converge to zero. When $t \geq 20$, the control signal $u(t)$ will converge to -4 which indicates that the output of the actuator $u^f(t) = 0.5u(t) + 2$ converges to zero. The trajectories of the parameter estimation variables $\hat{\Theta}(t)$, $\hat{\epsilon}(t)$ and $\hat{g}(t,x)$ are depicted in Figures 5 and 6, respectively. When $t \geq 20$ the estimation variable $\hat{\Theta}(t)$ will converge to the constant 0.314 and the estimation variable $\hat{\epsilon}(t)$ will converge to 1.245. It should be noted that although the actuator faults $u^f(t) = 0.5u(t) + 2$ and the unknown parameter $g(x)$ cannot be accurately estimated, the whole system can still be stabilized by the proposed FTC control scheme.

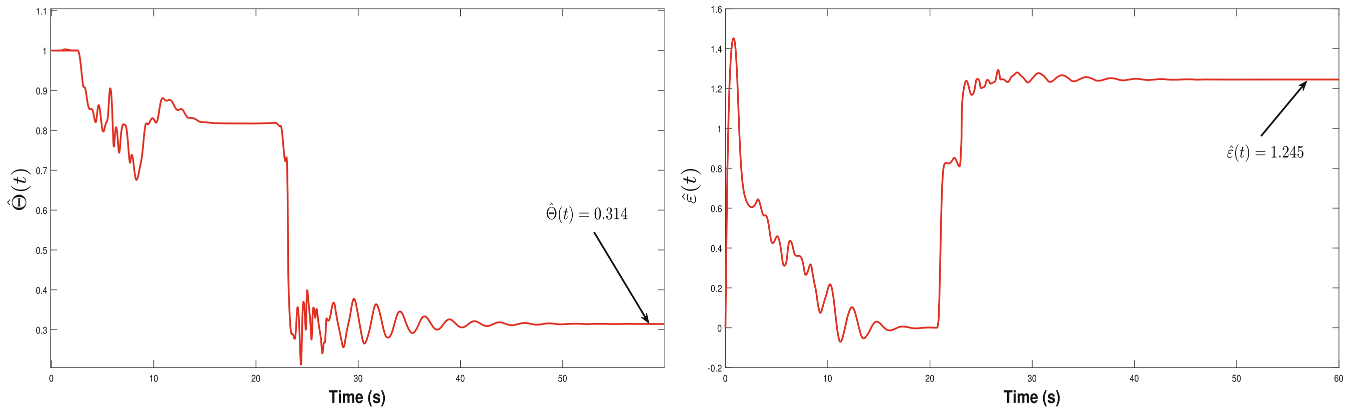

(A) (B)

FIGURE 5 Trajectories of the fault parameter estimations (A) $\hat{\Theta}(t)$ and (B) $\hat{\varepsilon}(t)$

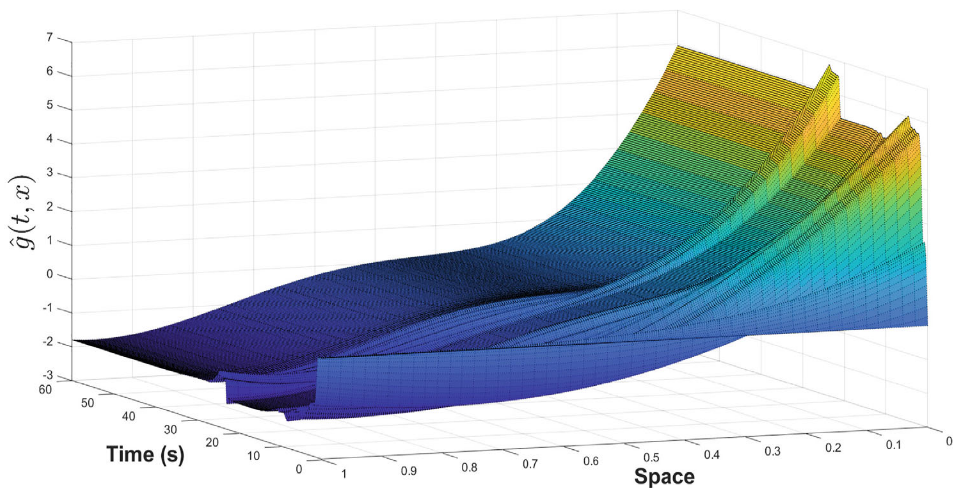

FIGURE 6 Trajectory of the parameter estimation $\hat{g}(t,x)$

6 | CONCLUSION

In this article, the output-feedback boundary adaptive FTC problem is addressed for scalar hyperbolic PDE system with actuator faults. The combined multiplicative and additive actuator faults are considered. The uncertainties of control system, which consist of both uncertain fault parameters and uncertain system parameters, are compensated by parameter updating laws of gradient type. With the filters based observer and the parameter updating laws, an output-feedback boundary adaptive fault-tolerant controller is designed via infinite-dimensional backstepping method. The pointwise boundedness of all the signals involved in the control design is guaranteed and the system state will converge to zero pointwise in space. The simulation studies validate that the proposed adaptive FTC control scheme can reduce the impact of the actuator faults.

ACKNOWLEDGMENTS

The authors are grateful to the Editor-in-Chief, the Associate Editor, and anonymous reviewers for their valuable and constructive comments based on which the presentation of this paper has been greatly improved.

FUNDING INFORMATION

This work was supported in part by the National Natural Science Foundation of China (U21B6001, 62173109, 61873311), the Special Project of Heilongjiang Postdoctoral Science Foundation (LBH-TZ2011), and the 111 Project (B16014).

ORCID

Tong Wang https://orcid.org/0000-0002-7252-1695

REFERENCES

1. Hao S, Xue H, Pan Y. Adaptive fuzzy dual-performance fault-tolerant control for interconnected nonlinear systems. *Int J Adapt Control Signal Process*. 2021;35(9):1685-1711.
2. Yang T, Li Y. Fixed-time fault-tolerant control for a class of switched nonlinear systems. *Int J Adapt Control Signal Process*. 2020;34(12):1768-1778.
3. Deng C, Wen C. Distributed resilient observer-based fault-tolerant control for heterogeneous multiagent systems under actuator faults and DoS attacks. *IEEE Trans Control Netw Syst*. 2020;7(3):1308-1318.
4. Gu Z, Yao L. Fault diagnosis and fault-tolerant control of uncertain network control systems. *Int J Adapt Control Signal Process*. 2021;35(9):1941-1956.
5. Van M, Ge S, Ren H. Finite time fault tolerant control for robot manipulators using time delay estimation and continuous nonsingular fast terminal sliding mode control. *IEEE Trans Cybern*. 2017;47(7):1681-1693.
6. Singh R, Bhushan B. A novel fault classification-based fault-tolerant control for two degree of freedom helicopter systems. *Int J Adapt Control Signal Process*. 2020;34(8):1080-1104.
7. Amin AA, Hasan KM. A review of fault tolerant control systems: advancements and applications. *Measurement*. 2019;143:58-68.
8. Zhao Q, Jiang J. Reliable state feedback control system design against actuator failures. *Automatica*. 1998;34(10):1267-1272.
9. Liao F, Wang J, Yang G. Reliable robust flight tracking control: an LMI approach. *IEEE Trans Control Syst Technol*. 2002;10(1):76-89.
10. Benosman M, Lum KY. Passive actuators' fault-tolerant control for affine nonlinear systems. *IEEE Trans Control Syst Technol*. 2010;18(1):152-163.
11. Maki M, Jiang J, Hagino K. A stability guaranteed active fault-tolerant control system against actuator failures. *Int J Robust Nonlinear Control*. 2004;14(12):1061-1077.
12. Li X, Wang J. Active fault-tolerant consensus control of Lipschitz nonlinear multiagent systems. *Int J Robust Nonlinear Control*. 2020;30(13):5233-5252.
13. Jiang J, Yu X. Fault-tolerant control systems: a comparative study between active and passive approaches. *Annu Rev Control*. 2012;36(1):60-72.
14. Jin X, Lu S, Qin J, Zheng W. Auxiliary constrained control of a class of fault-tolerant systems. *IEEE Trans Syst Man Cybern Syst*. 2021;51(4):2272-2283.
15. Xiao B, Hu Q, Zhang Y. Adaptive sliding mode fault-tolerant attitude tracking control for flexible spacecraft under actuator saturation. *IEEE Trans Control Syst Technol*. 2012;20(6):1605-1612.
16. Chen M, Shi P, Lim C. Adaptive neural fault-tolerant control of a 3-DOF model helicopter system. *IEEE Trans Syst Man Cybern Syst*. 2016;46(2):260-270.
17. Wang T, Qiu J, Gao H. A combined fault-tolerant and predictive control for network-based industrial processes. *IEEE Trans Ind Electron*. 2016;63(4):2529-2536.
18. Liu L, Wang D, Peng Z, Han Q-L. Distributed path following of multiple under-actuated autonomous surface vehicles based on data-driven neural predictors via integral concurrent learning. *IEEE Trans Neural Netw Learn Syst*. 2021. doi:10.1109/TNNLS.2021.3100147
19. Li Y, Liu Y, Tong S. Observer-based neuro-adaptive optimized control for a class of strict-feedback nonlinear systems with state constraints. *IEEE Trans Neural Netw Learn Syst*. 2021. doi:10.1109/TNNLS.2021.3051030
20. Gao H, Song Y, Wen C. Backstepping design of adaptive neural fault-tolerant control for MIMO nonlinear systems. *IEEE Trans Neural Netw Learn Syst*. 2017;28(11):2605-2613.
21. Shen Q, Jiang B, Cocquempot V. Adaptive fuzzy observer-based active fault-tolerant dynamic surface control for a class of nonlinear systems with actuator faults. *IEEE Trans Fuzzy Syst*. 2014;22(2):338-349.
22. Li Y, Sun K, Tong S. Observer-based adaptive fuzzy fault-tolerant optimal control for SISO nonlinear systems. *IEEE Trans Cybern*. 2019;49(2):649-661.
23. Sun K, Liu L, Qiu J, Feng G. Fuzzy adaptive finite-time fault-tolerant control for strict-feedback nonlinear systems. *IEEE Trans Fuzzy Syst*. 2021;29(4):786-796.
24. Anfinsen H, Aamo OM. *Adaptive Control of Hyperbolic PDEs*. Springer; 2019.
25. Smyshlyaev A, Krstic M. *Adaptive Control of Parabolic PDEs*. Princeton University; 2010.
26. Smyshlyaev A, Krstic M. Closed-form boundary state feedbacks for a class of $1-D$ partial integro-differential equations. *IEEE Trans Automat Contr*. 2004;49(12):2185-2202.
27. Deutscher J. Backstepping design of robust output feedback regulators for boundary controlled parabolic PDEs. *IEEE Trans Automat Contr*. 2016;61(8):2288-2294.
28. Krstic M, Smyshlyaev A. Backstepping boundary control for first-order hyperbolic PDEs and application to systems with actuator and sensor delays. *Syst Control Lett*. 2008;57(9):750-758.
29. Vazquez R, Krstic M, Coron JM. Backstepping boundary stabilization and state estimation of a 2×2 linear hyperbolic system. Proceedings of the 50th IEEE Conference on Decision and Control and European Control Conference; 2011; 4937-4942.
30. Smyshlyaev A, Guo B, Krstic M. Arbitrary decay rate for Euler-Bernoulli beam by backstepping boundary feedback. *IEEE Trans Automat Contr*. 2009;54(5):1134-1140.

31. Deutscher J, Gehring N, Kern R. Output feedback control of general linear heterodirectional hyperbolic ODE-PDE-ODE systems. *Automatica*. 2018;95:472-480.
32. de Andrade GA, Vazquez R, Pagano DJ. Backstepping stabilization of a linearized ODE-PDE Rijke tube model. *Automatica*. 2018;96:98-109.
33. Krstic M, Smyshlyaev A. Adaptive boundary control for unstable parabolic PDEs Part I: Lyapunov design. *IEEE Trans Automat Contr*. 2008;53(7):1575-1591.
34. Xu Z, Liu Y. Adaptive boundary stabilization for first-order hyperbolic PDEs with unknown spatially varying parameter. *Int J Robust Nonlinear Control*. 2016;26(3):613-628.
35. Krstic M, Smyshlyaev A. Adaptive boundary control for unstable parabolic PDEs part II: estimation-based designs. *Automatica*. 2007;43(9):1543-1556.
36. Krstic M, Smyshlyaev A. Adaptive boundary control for unstable parabolic PDEs Part III: output feedback examples with swapping identifiers. *Automatica*. 2007;43(9):1557-1564.
37. Bernard P, Krstic M. Adaptive output-feedback stabilization of non-local hyperbolic PDEs. *Automatica*. 2014;50(10):2692-2699.
38. Anfinsen H, Aamo OM. Adaptive stabilization of 2×2 linear hyperbolic systems with an unknown boundary parameter from collocated sensing and control. *IEEE Trans Automat Contr*. 2017;62(12):6237-6249.
39. Ji N, Liu J. Adaptive actuator fault-tolerant control for a three-dimensional Euler Bernoulli beam with output constraints and uncertain end load. *J Franklin Inst*. 2019;356(7):3869-3898.
40. Ji N, Liu J. Observer-based fuzzy fault-tolerant control for nonlinear parabolic PDEs. *Int J Fuzzy Syst*. 2020;22:111-121.
41. Ghantasala S, El-Farra NH. Active fault tolerant control of sampled data nonlinear distributed parameter systems. *Int J Robust Nonlinear Contr*. 2012;22(1):24-42.
42. Liu Z, Liu J, He W. Robust adaptive fault tolerant control for a linear cascaded ODE-beam system. *Automatica*. 2018;98:42-50.
43. Xu X, Yuan Y, Wang M, Fu M, Dubljevic S. Fault detection and estimation for a class of PIDE systems based on boundary observers. *Int J Robust Nonlinear Control*. 2019;29(17):5867-5885.
44. Cai J, Ferdowsi H, Sarangapani J. Model-based fault detection, estimation, and prediction for a class of linear distributed parameter systems. *Automatica*. 2016;66:122-131.
45. Guang YC, Yang H, Jiang B. Fault-tolerant control for a class of switched linear hyperbolic systems. *Int J Control*. 2019;4(94):871-880.
46. Yang WY, Cao W, Chung TS, Morris J. *Applied Numerical Methods Using Matlab*. John Wiley; 2005.

How to cite this article: Guo R, Li J, Sun K, Wang T, Qiu J. Output-feedback boundary adaptive fault-tolerant control for scalar hyperbolic partial differential equation systems with actuator faults. *Int J Adapt Control Signal Process*. 2022;36(11):2716-2731. doi: 10.1002/acs.3478